ORIGINAL RESEARCH

Probabilistic Presurgical Language Functional MRI Atlas of Brain Tumor Patients

Jian Ming Teo, Vinodh A. Kumar, Jina Lee, Rami W. Eldaya, Ping Hou, Mu-Lan Jen, Kyle R. Noll, Peng Wei, Sherise D. Ferguson, Sujit S. Prabhu, Max Wintermark, and Ho-Ling Liu

ABSTRACT

BACKGROUND AND PURPOSE: Patients with brain tumors have high intersubject variation in putative language regions, which may limit the utility of straightforward application of healthy-subject brain atlases in clinical scenarios. The purpose of this study was to develop a probabilistic functional brain atlas that consolidates language functional activations of sentence completion and silent word generation language paradigms using a large sample of patients with brain tumors.

MATERIALS AND METHODS: The atlas was developed using retrospectively collected fMRI data from patients with brain tumors who underwent their first standard-of-care presurgical language fMRI scan at our institution between July 18, 2015, and May 13, 2022. 317 patients (861 fMRI scans) were used to develop the language functional atlas. An independent presurgical language fMRI dataset of 39 patients with brain tumors from a previous study was used to evaluate our atlas. Family-wise error corrected binary functional activation maps from sentence completion, letter fluency, and category fluency presurgical fMRI were used to create probability overlap maps and pooled probabilistic overlap map in Montreal Neurological Institute standard space. Wilcoxon signed-rank test was used to determine significant difference in the maximum Dice coefficient for our atlas compared to a meta-analysis-based template with respect to expert-delineated primary language area activations.

RESULTS: Probabilities of activating left anterior primary language area and left posterior primary language area in temporal lobe were 87.9% and 91.5%, respectively, for sentence completion, 88.5% and 74.2%, respectively, for letter fluency, and 83.6% and 67.6%, respectively, for category fluency. Maximum Dice coefficients for templates derived from our language atlas were significantly higher than the meta-analysis-based template in left anterior primary language area (0.351 and 0.326, respectively, $P < .05$) and left posterior primary language area in temporal lobe (0.274 and 0.244, respectively, $P < .005$).

CONCLUSIONS: Brain tumor patient- and paradigm-specific probabilistic language atlases were developed. These atlases had superior spatial agreement with fMRI activations in individual patients than the meta-analysis-based template.

ABBREVIATIONS: SENT = sentence completion, LETT = letter fluency, CAT = category fluency, PLA = primary language area, aPLA = anterior PLA, $pPLA_T$ = posterior PLA in the temporal lobe, $pPLA_P$ = posterior PLA in the parietal lobe, SMA = supplementary motor area, DLPFC = dorsolateral prefrontal cortex, BTLA = basal temporal language area

Received month day, year; accepted after revision month day, year.
From the Department of Imaging Physics (JM.T,P.H,ML.J,HL.L), Department of Diagnostic Radiology (V.A.K, J.L, R.W.E, M.W), Department of Neuro-Oncology (K.R.N), Department of Biostatistics (P.W), Department of Neurosurgery (S.D.F, S.P), The University of Texas MD Anderson Cancer Center, Houston, TX, USA; Medical Physics Graduate Program (JM.T), The University of Texas MD Anderson Cancer Center UTHealth Graduate School of Biomedical Sciences, Houston, TX, USA.

The authors declare no conflicts of interests related to the content of this article.

Please address correspondence to Ho-Ling Liu, Ph.D, Department of Imaging Physics, Division of Diagnostic Imaging, The University of Texas MD Anderson Cancer Center, 1515 Holocombe Blvd, Houston, TX, 77030, USA, HLALiu@mdanderson.org

SUMMARY SECTION

PREVIOUS LITERATURE: The analysis of language fMRI data acquired from brain tumor patients is typically supported by atlases developed from predominantly healthy subjects. However substantial intersubject in brain tumor patients may adversely affect the utility of straightforward application of such atlases. While disease-specific population-based structural brain atlases have been developed from MRI data, there is no atlas developed using functional imaging data, specifically language data, from a sizable disease-specific population.

KEY FINDINGS: Significantly better spatial agreement with expert-delineated language activations in individual brain tumor patients was found for templates generated from probabilistic language atlas developed using brain tumor patients compared to a meta-analysis-based template. Probabilities of each activating primary and ancillary languages areas in both hemispheres were determined for clinical language paradigms.

KNOWLEDGE ADVANCEMENT: Development of probabilistic language atlas based on clinical language fMRIs of brain tumor patients with potential clinical and research applications in language laterality assessment, network categorization and biomarker discovery.

INTRODUCTION

Brain atlases provide a common framework to interpret, communicate, and use large amounts of neuroimaging data after accounting for individual differences[1]. Our current understanding of the human brain suggests that structural anatomy alone is insufficient to explain

functional characteristics[2]; hence, functional atlases play a crucial role in consolidating and advancing current research on brain function[3, 4]. Clinically, atlases of canonical language or other functional areas have been used for laterality assessment[5], network categorization[6], and biomarker discovery[7]. Such applications leverage atlases developed from healthy individuals, although patients with brain diseases have significant variations in brain anatomy and functions. While disease-specific population-based structural brain atlases have been previously developed from MRI data[8], currently, there is no atlas developed using functional imaging data, specifically language data, from a sizable disease-specific population.

For patients with brain tumors, studies have demonstrated substantial intersubject variation in putative language regions, which can be attributed to tumor infiltration and surrounding edema promoting cortical reorganization and functional displacement[9-11]. Thus, straightforward applications of atlases developed using data from healthy individuals may have limited utility in patients with brain tumors. In the last two decades, functional MRI has emerged as the standard of care in many institutions for localizing eloquent cortices and lateralizing language functions for preoperative planning of brain tumor surgery[12, 13]. Given the availability of preoperative fMRI data and the use of increasingly standardized procedures[14, 15], it is possible to assemble fMRI-based functional atlases that consider the intersubject variation of patients with brain tumors.

Because language is multifaceted (phonologic, semantic, etc.) and involves a highly complex network of brain areas[16, 17], functional mapping results can vary with the language task, task paradigm, and patient performance. For preoperative fMRI, studies have advocated for the use of multiple task paradigms to generate reliable and accurate activation of language networks[18, 19]. To alleviate widespread variability in clinical practice, the American Society of Functional Neuroradiology recommends standard sets of language paradigms, with the top two types of paradigms being sentence completion and silent word generation for adult patients[15].

This study aimed to develop a probabilistic functional brain atlas to consolidate language activations from these two types of paradigms in patients with brain tumors. For evaluation, templates of anterior and posterior primary language areas (PLAs) were generated from the atlas and compared to a meta-analysis-based template[20] by their spatial similarity with a separate dataset of presurgical fMRI studies.

MATERIALS AND METHODS

Subjects

This retrospective study was approved by the institutional review board at our institution, and the requirement for patient informed consent was waived. Initially, 324 patients who had undergone their first standard-of-care presurgical language fMRI between July 18, 2015, and May 13, 2022, were considered. Each fMRI study included at least one of the three paradigms: sentence completion (SENT), letter fluency (LETT), and category fluency (CAT). Patients with head motion exceeding 2 mm translation or 2° rotation were excluded in proceeding analysis. In total, 7 patients were excluded due to incomplete data (n = 3) or not having any language fMRI scans that met our head motion criteria (n = 4), leading to 317 included patients (183 male and 134 female; mean age, 51±16 years) with 861 fMRI scans for generating the language atlases (See Supplementary Table 1 for patient demographic and clinical characteristics). These fMRI scans consisted of SENT from 281 patients (157 male and 124 female; mean age, 50±16 years), CAT from 293 patients (169 male and 124 female; mean age, 50±16 years), and LETT from 287 patients (166 male and 121 female; mean age, 50±16 years).

For evaluation, we used a separate fMRI dataset from a previous study that included 39 patients with brain tumors (22 male and 17 female; mean age, 48±15 years)[21]. This dataset, which includes 38 SENT and 34 LETT fMRI scans, was acquired at our institution using identical acquisition protocols and task paradigms.

Image Acquisition

All MRI scans were performed on 3T clinical scanners (GE HealthCare, Milwaukee, WI). fMRI scans were acquired using a T2*W gradient-echo EPI sequence (TR/TE = 2000 ms/25 ms; Flip angle = 90 degrees; Parallel imaging acceleration factor = 2; 32 slices with 4-mm thickness and no gap; in-plane resolution = 3.75 × 3.75 mm^2; Duration = 4 minutes). Anatomic images were obtained using a 3D T1W inversion recovery-prepared spoiled gradient-echo sequence (TR/TE/TI = 6.1/2.1/400 ms; Flip angle = 20 degrees; 1.0 x 1.0 x 1.2 mm^3 voxel) and a T2W FLAIR sequence (TR/TE/TI = 10000/142/2250 ms; 1.0 x 1.0 x 2.0 mm^3 voxel).

Language paradigms included 6 cycles of 20-second control and 20-second task blocks. For SENT, task blocks consisted of incomplete sentences and patients were tasked to think of a word to be filled into a blank. For SENT control blocks, patients were shown four gibberish sentences in a format resembling that in the active block. For LETT task blocks, patients were shown a letter and tasked to covertly generate words beginning with that letter. For CAT task blocks, patients were shown a category (e.g., animals or types of food) and tasked to covertly generate words related to the category. For LETT and CAT control blocks, patients were asked to tap their fingers on their thumb bilaterally. The paradigms were displayed with an MRI-compatible liquid crystal display (Invivo SensaVue, Phillips).

Image Analysis and Atlas Construction

Image analyses were performed using AFNI[22] (for individual fMRI analysis except for spatial normalization), SPM12 (https://www.fil.ion.ucl.ac.uk/spm/software/spm12/) (for spatial normalization), and in-house Python scripts[23]. fMRI preprocessing included motion correction, slice timing correction, co-registration with 3D T1-weighted images, spatial normalization to Montreal Neurological Institute (MNI) space, and spatial smoothing with an isotropic 6-mm width at half-maximum Gaussian kernel. General linear model with a canonical hemodynamic response function was used to generate t-value activation maps. Significantly activated clusters ($P < .05$, family-wise error corrected) were determined using AFNI 3dClustSim to obtain the cluster threshold at the uncorrected cluster-forming threshold of $P < .0001$. The thresholded t-value map was then binarized to form an activation mask for each fMRI scan.

Language atlases for each paradigm were obtained as probabilistic overlap maps (POMs) by adding binary activation masks and divided by number of contributing patients. A probabilistic language atlas was also calculated as a pooled POM by adding all binary activation masks across the three paradigms divided by the total number of fMRI scans used.

Probability of fMRI Paradigms Activating Language Areas

Automated Anatomical Labelling Atlas 3[24] was applied to determine the probability that each fMRI paradigm activated language-related regions of interest (ROIs) after spatial transformation to the MNI space [25] using Advanced Normalization Tools[26]. The following ROIs were studied (see Supplementary Table 2): anterior PLA (aPLA), posterior PLA in the temporal lobe ($pPLA_T$), posterior PLA in the parietal lobe ($pPLA_P$), supplementary motor area (SMA), dorsolateral prefrontal cortex (DLPFC), basal temporal language area (BTLA), and insula. For each paradigm, the probability of detecting activation within each ROI was determined as the percentage of patients having activated cluster(s) overlapping with the ROI.

Comparison with a Meta-analysis-based Template

PLA templates from the atlas were generated and compared with a meta-analysis-based language template by its spatial similarity to fMRI activations in a separate fMRI dataset of 39 brain tumor patients. The templates were generated by constraining the pooled probabilistic language atlas with the anatomical aPLA and $pPLA_T$ ROIs described above. The meta-analysis-based language template was obtained from a Neurosynth result of 1101 fMRI studies with the same anatomical constraints[20].

Details of the separate fMRI dataset were described in a previous study[21]. Briefly, after standard fMRI processing, two board-certified neuroradiologists with expertise in clinical fMRI outlined significantly activated areas in the aPLA (focusing on the posterior inferior frontal gyrus, including the pars triangularis and pars opercularis) and $pPLA_T$ (focusing on the posterior superior temporal gyrus and posterior middle temporal gyrus). Variations in anatomy and fMRI cluster distribution were considered on an individual patient basis. In total, 62 aPLA and 61 $pPLA_T$ activation maps were obtained.

Dice coefficient was used to evaluate the spatial similarity between the templates and the activation maps of the separate patient datasets within the anatomical ROIs of aPLA and $pPLA_T$. We varied the thresholds of the two templates at fixed intervals (.1% for the probabilistic atlas-based template; maximum z-score/1000 for the meta-analysis-based template), and Dice coefficients were calculated for each thresholded template. The maximum Dice coefficient across thresholds was used for comparison.

Statistical Analysis

Wilcoxon signed-rank tests were performed to determine significant differences between templates in maximum Dice coefficient. Statistical analyses were conducted with scipy.stats.wilcoxon (Python 3.8.13, Scipy 1.8.1). A p-value of less than .05 was considered statistically significant.

RESULTS

Language Atlases from Individual Paradigms

The language atlases from individual paradigms are illustrated in Fig 1. Consistently across the three paradigms, the left aPLA, left DLPFC, left SMA, and right cerebellum had high probability of overlap. Among the three paradigms, SENT had voxels with higher probability of overlap in the left $pPLA_T$ (Fig 1A), while CAT had voxels with higher overlap in the occipital lobe (Fig 1C).

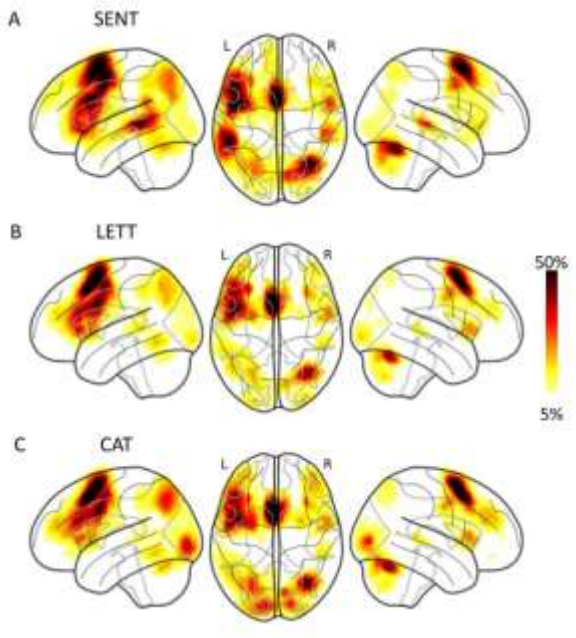

FIG 1. Language functional atlases based on probabilistic overlap maps of individual paradigms. The atlases are presented using glass brain projection. L = left hemisphere; R = right hemisphere; SENT = sentence completion; LETT = letter fluency; CAT = category fluency.

Probability of fMRI Paradigms Activating Language Areas

Table 1 presents the probabilities of activating in each of the ROIs with the SENT, LETT, and CAT paradigms. Generally, across the three paradigms, greater probabilities of activating were found in the left hemisphere than in the right hemisphere. All three paradigms had greater than 80% probability of activating areas in the left aPLA, left DLPFC, and left and right SMA, whereas only SENT had greater than 80% probability of activating the left $pPLA_T$ and only CAT had greater than 80% probability of activating right DLPFC. In the left $pPLA_T$ and $pPLA_P$, SENT had noticeably higher probabilities (91.5% and 76.9%, respectively) than did LETT (74.2% and 53.0%, respectively) and CAT (67.6% and 56.0%, respectively).

Table 1: Probability of Activation Across Three Language Paradigms

Probability of Activation (%)						
Paradigm	SENT		LETT		CAT	
ROI	L	R	L	R	L	R
aPLA	87.9	61.2	88.5	62.4	83.6	74.1
$pPLA_T$	91.5	66.9	74.2	48.8	67.6	47.8
$pPLA_P$	76.9	39.9	53.0	30.3	56.0	39.2
SMA	90.7	84.0	91.6	90.6	94.5	90.4
DLPFC	94.3	63.0	89.5	69.3	91.5	84.6
BTLA	68.0	65.5	55.7	57.5	68.3	63.5
Insula	59.4	43.8	65.9	51.2	59.7	52.6

Abbreviations: ROI = region of interest; aPLA = anterior primary language area; $pPLA_T$ = posterior primary language area in temporal lobe; $pPLA_P$ = posterior primary language area in parietal lobe; SMA = supplementary motor area; DLPFC = dorsolateral prefrontal cortex; BTLA = basal temporal language area; L = left hemisphere; R = right hemisphere; SENT = sentence completion; LETT = letter fluency; CAT = category fluency.

Probabilistic Language Atlas

The probabilistic language atlas, built based on a pooled POM that consisted of activation maps from 861 language fMRI scans, is presented in Fig 2 as a penetrance map. The left hemisphere had, overall, more extensive and higher overlap probability in the atlas than right hemisphere. PLAs and ancillary language areas, including aPLA, $pPLA_T$, $pPLA_P$, pre-SMA, DLPFC, BTLA, and insula, were clearly identified with a 5% probability threshold (Fig. 2). The regions containing voxels with 40% or greater probability of overlap included the left aPLA, left DLPFC, and pre-SMA. Peak probabilities of overlap for left $pPLA_T$ and $pPLA_p$ were 24% and 12%, respectively.

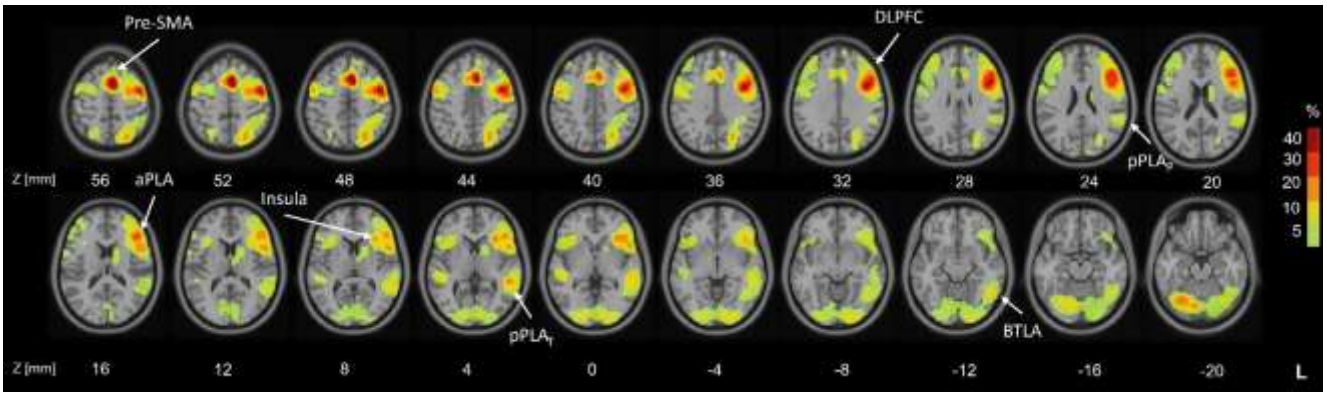

FIG 2. Pooled probabilistic language functional atlas presented as a penetrance map overlaid on T1-weighted standard MNI brain images. Z = MNI coordinate of each axial slice in mm. aPLA = anterior primary language area; $pPLA_T$ = posterior primary language area in temporal lobe; $pPLA_P$ = posterior primary language area in parietal lobe; pre-SMA = pre-supplementary motor area; DLPFC = dorsolateral prefrontal cortex; BTLA = basal temporal language area.

Comparison with the Meta-analysis-based Template

Fig 3 presents boxplots comparing the maximum Dice coefficients between the PLA activations of the evaluation fMRI dataset and the PLA templates derived from the probabilistic language atlas vs. the Neurosynth meta-analysis-based results obtained from varying thresholds for the templates. The maximum Dice coefficients for templates derived from the probabilistic language atlas were significantly higher than those for the meta-analysis-based templates both in aPLA (0.351 and 0.326, respectively, $P < .05$) and in $pPLA_T$ (0.274 and

0.244, respectively, $P < .005$). Fig 4 illustrates the fMRI activations and templates on overlaid on T2 FLAIR images of two representative patients. Both patient A and B have glioblastoma in the left frontal lobe. At the threshold with maximum Dice coefficient, the template from the probabilistic language atlas had noticeably better spatial agreement with $pPLA_T$ activations in patient A. For patient B, the template derived from the probabilistic language atlas demonstrated better spatial agreement with both aPLA and $pPLA_T$ activations.

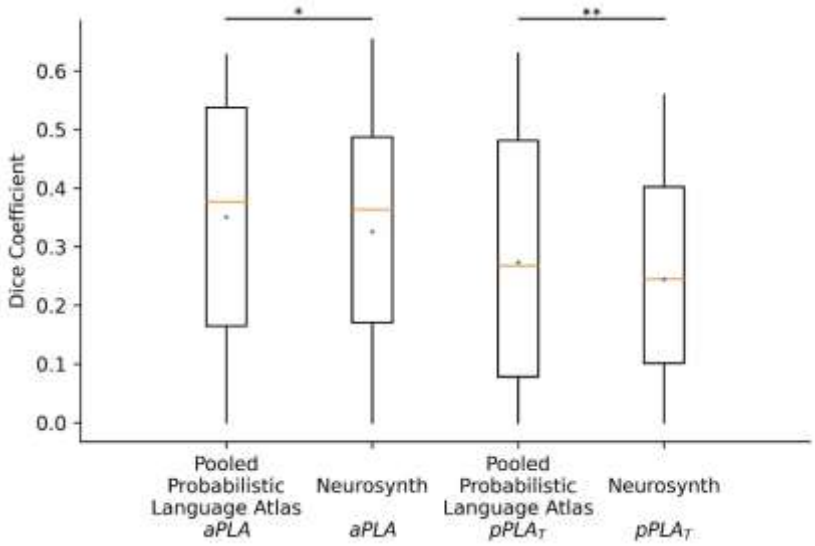

FIG 3. Box plots of maximum Dice coefficient for probabilistic language atlas-derived vs Neurosynth-derived templates. Dice coefficients were calculated across thresholds for each template with respect to each individual's activations in aPLA and $pPLA_T$. Maximum Dice coefficient across thresholds was used to construct the box plot. Horizontal orange lines indicate median values, and blue dots indicate mean values among subjects (n=39). aPLA = anterior primary language area; $pPLA_T$ = posterior primary language area in temporal lobe. *P < .05. **P < .005.

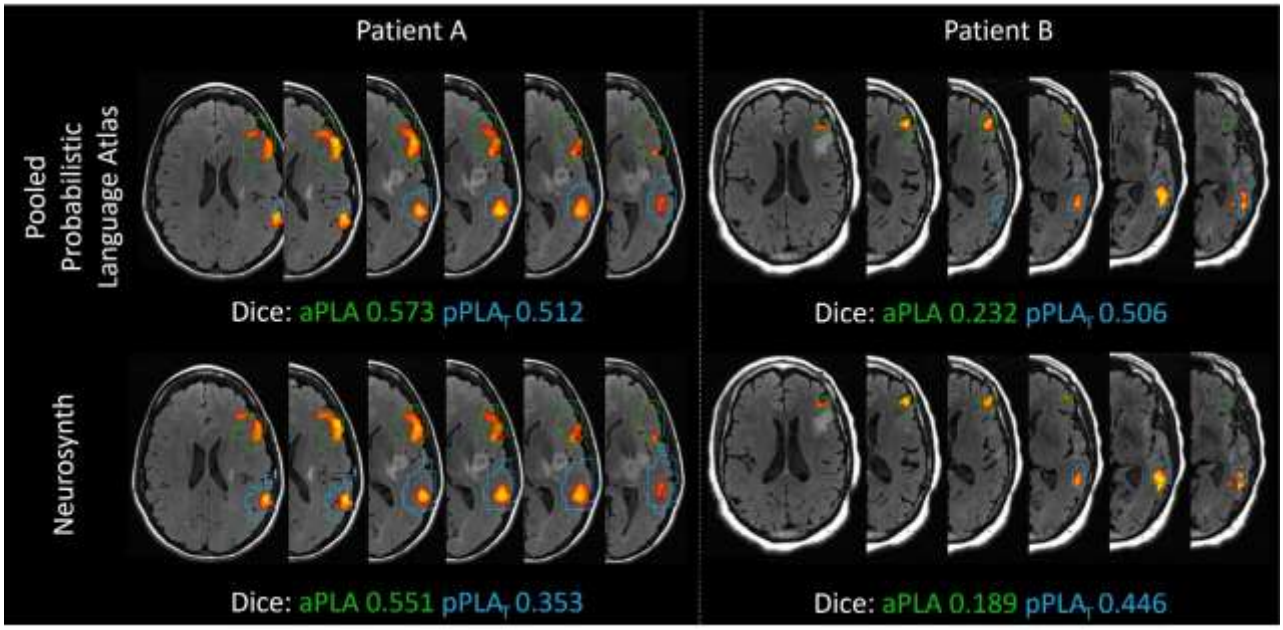

FIG 4. Sentence completion fMRI activations and the language templates in anterior primary language area (aPLA) and posterior PLA in temporal lobe ($pPLA_T$) overlaid on T2 FLAIR images of two representative patients. Significant fMRI activations (P<0.05, FWE corrected) are displayed with color blobs ranging from red to yellow. Green and blue contours outline the probabilistic language atlas- (top) and Neurosynth-based (bottom) templates at maximum dice coefficients for the aPLA and the $pPLA_T$, respectively.

DISCUSSION

Language atlases provide templates for quantitative assessment of language mapping, such as localization, lateralization, and strength, as well as for automated detection of language networks with resting-state fMRI [5-7]. This study presents the first language atlas built from preoperative fMRI results of patients with brain tumors using the language paradigms similar to those recommended by the American Society of Functional Neuroradiology (i.e., sentence completion and silent word generation) [15].

Although patients with brain tumors can have discernible intersubject variation in functional activations, language atlases from this study involve a large number of fMRI activations projected onto a standard space. Thus, we were able to reproduce known characteristics of the language network. For example, critical language regions that are commonly assessed clinically, such as Broca's area (aPLA), Wernicke's area ($pPLA_T$), angular and supramarginal gyrus ($pPLA_P$), DLPFC, pre-SMA, and BTLA can be observed[18, 27, 28]. Left-hemisphere dominance is still observed considering the higher probability of overlap in left-hemisphere PLAs and ancillary language areas compared to their right-hemisphere counterparts[27, 28].

In agreement with the literature, we observed that the semantic task (SENT) was more likely to activate posterior PLAs compared to the two silent word generation tasks (CAT and LETT)[15, 29]. This can be attributed to sentence completion tasks being more proficient at activating the posterior language network[29, 30]. Across all three paradigms, the higher probability of overlap in $pPLA_T$ compared to that of $pPLA_P$ agrees with a previous study of language regions in presurgical fMRI[18]. We also found that the probability of detecting activation in the right DLPFC for the CAT task was higher than that of the SENT and LETT tasks. This finding can be attributed to more likely recruitment of the right DLPFC for the CAT task, which is corroborated by a separate study on verbal fluency paradigms[31], and to the involvement of the right DLPFC in retrieval tasks[32]. The probability of detecting activation in the SMA for both hemispheres was similar across the three paradigms, a likely consequence of the intersubject variation during spatial normalization and the 6 mm isotropic smoothing applied during preprocessing. Considering that SMA laterality is known to corroborate language laterality[5], it can still be observed that the spatial extent of SMA activations is asymmetric towards the left hemisphere on the POM.

The pooled probabilistic language atlas developed in this study is equivalent to the weighted average of the three language paradigm POMs. As such, the pooled probabilistic language atlas developed in this study emphasizes areas of activation common across the three paradigms. Based on use case and context, the pooling strategy and choice of paradigms to include can differ. Thus, we had also created language atlases from single paradigms and made them available. The distinguishing attribute between our language atlases and others developed from healthy individuals is its information on intersubject variation. In our atlases, this difference is encapsulated by the spatial extent of the atlas at a specified overlap threshold, with higher thresholds corresponding to a lower tolerance for variation. For example, the spatial extent of areas with higher overlap in the frontal lobe is continuous between the proximally close aPLA and DLPFC in the left hemisphere and can be attributed to using a population of patients with brain tumors for atlas building; these patient populations are to be heterogeneous in terms of functional anatomy[9]. Given the implementation of the POM methodology, sources of inter-subject variation taken into consideration include intrinsic variation, normalization imprecision due to lesion-distorted anatomy, and functional reorganization due to tumor invasion.

We compared our results with those of Neurosynth because it is a widely-referenced large-scale platform for automated synthesis of fMRI data. The Neurosynth result is a statistical inference map generated using a chi-square test of independence and informs if a voxel's coordinates have been reported more consistently in studies involving the term "language" than in studies that did not[20]. Therefore, it allowed us to calculate Dice coefficients in a similar fashion among varying thresholds to ensure a fair comparison. The comparison demonstrated that our templates had better agreement with individual patient's fMRI. This may be attributed to the Neurosynth meta-analysis including fMRI studies with different cohorts, primarily healthy individuals, various task and resting-state fMRI paradigms, and different acquisition and analysis methods, whereas our atlas was built from a uniform source of fMRI data. In addition, for patients with brain tumors, the position of a tumor with respect to the classic/principal functional anterior-Broca and posterior-Wernicke areas can influence the locoregional functional reorganization. Given the quite large group of patients included in the study, it is possible that filtering for contributing patients with similar tumor locations (e.g. anterior or posterior) during atlas development may allow for better spatial agreement with the evaluation dataset.

We envision our atlas to have potential clinical and research applications through the derivation of templates for ROIs. An example would be language assessment of patients with brain tumors in which templates of functional ROIs atlases based on healthy individuals are often used to calculate the laterality index. Templates generated from our atlas account for functional anatomy distortions due to the tumor, which may improve the fidelity of the calculated laterality index[5, 33]. Another example is imaging biomarker studies, wherein post-warping of primary and ancillary language areas into patient space, they can serve as language localizers for quantifying imaging measures, whether from fMRI activations of more specific paradigms, or different MRI sequences, or different imaging modalities[34, 35]. Our atlas could also be used to guide resting-state fMRI template matching for detecting language networks[6, 36] These applications could rely on manual delineation of language areas by experts, but atlases help to make the process automated and less operator dependent. The potential clinical implications of this study will depend on the improvement with each different use of the atlas, e.g. more accurate assessment of language lateralization, imaging biomarker quantification, or rs-fMRI language mapping. Further validation studies and clinical trials may be needed to assess the practicality and effectiveness of the atlas in clinical settings. Although the existence of large lesions and distorted anatomy may introduce potential inaccuracy of spatial registration[37], recent studies have demonstrated that such errors are reduced with more modern deformable registration methods allowing for reasonably good performance even in patients with brain tumors[38]. In addition, for large ROIs such as PLAs, the misregistration may remain local and its effect would be specific to applications (e.g., laterality calculation, biomarker quantification, template matching). If the ROI is far from the tumor, e.g. using anterior PLA atlas to calculate the laterality index for patient's tumor near posterior PLA, the effect of spatial registration should be minimum. If the use of atlas directly focuses on the language ROI covering/adjacent to lesions, we would recommend the users inspect the registration closely. Again, since the ROIs are with large spatial extents, the overall effect may not be significant. However, when there are concerns, one may consider extending the ROIs by applying a lower probability threshold on the atlas. This is one of the advantages of the probabilistic atlas.

This study presents some limitations. First, this is a single-institution study with MRI data gathered from limited scanner platforms. The dataset reflects the typical patient population undergoing presurgical fMRI in our institution. Including data from other institutions, which would incorporate more diverse patient cohorts and/or fMRI paradigms/method, could further refine the atlas. In parallel, multicenter studies have shown that fMRI data acquired on different scanners will have different activation effect size and spatial smoothness[39]. This may impact the atlas on areas with lower overlap probabilities (extents). However, we expect that the central tendencies

of high overlap probabilities to remain similar and corresponding brain regions identified in our atlas would still be useful for appropriate language-related analyses. Second, our atlas was developed using only data from patients with brain tumors. But it is worthwhile to note that a substantial portion of presurgical fMRI studies are performed for patients requiring brain tumor resection[40]. Third, only clinical language generation (LETT and CAT) and semantic paradigms (SENT) were used to develop the atlas. Thus, the functional anatomy typically recruited in these tasks is emphasized in our atlas. Other fMRI task paradigms may yield different weightings in language areas and may involve additional brain regions. The potential implications of this variation would likely depend on its application and whether the weights and the additional regions are used, e.g. for assessing language lateralization or for assisting rs-fMRI analysis.

CONCLUSIONS

In conclusion, we have developed probabilistic language atlases comprising of 861 presurgical language fMRI scans from 317 patients with brain tumors. Three paradigms were used in our study, and probabilities of each activating primary and ancillary languages areas in both hemispheres were determined. We found significantly better spatial agreement with expert-delineated language activations in individual patients for the PLA templates generated from our atlas to a meta-analysis-based template.

ACKNOWLEDGMENTS

This study was supported by NIH/NCI under award number R01 CA258788 and P30 CA016672. Editorial support was provided by Research Medical Library at University of Texas MD Anderson Cancer Center.

REFERENCES

1. Van Essen DC. Windows on the brain: the emerging role of atlases and databases in neuroscience. *Curr Opin Neurobiol* 2002;12:574-579
2. Honey CJ, Sporns O, Cammoun L, et al. Predicting human resting-state functional connectivity from structural connectivity. *Proc Natl Acad Sci U S A* 2009;106:2035-2040
3. Lipkin B, Tuckute G, Affourtit J, et al. Probabilistic atlas for the language network based on precision fMRI data from >800 individuals. *Sci Data* 2022;9:529
4. Yeo BT, Krienen FM, Sepulcre J, et al. The organization of the human cerebral cortex estimated by intrinsic functional connectivity. *J Neurophysiol* 2011;106:1125-1165
5. Agarwal S, Hua J, Sair HI, et al. Repeatability of language fMRI lateralization and localization metrics in brain tumor patients. *Hum Brain Mapp* 2018;39:4733-4742
6. Branco P, Seixas D, Deprez S, et al. Resting-State Functional Magnetic Resonance Imaging for Language Preoperative Planning. *Front Hum Neurosci* 2016;10:11
7. Abraham A, Milham MP, Di Martino A, et al. Deriving reproducible biomarkers from multi-site resting-state data: An Autism-based example. *Neuroimage* 2017;147:736-745
8. Thompson PM, Mega MS, Woods RP, et al. Cortical change in Alzheimer's disease detected with a disease-specific population-based brain atlas. *Cereb Cortex* 2001;11:1-16
9. Sanai N, Mirzadeh Z, Berger MS. Functional outcome after language mapping for glioma resection. *N Engl J Med* 2008;358:18-27
10. Lawrence A, Carvajal M, Ormsby J. Beyond Broca's and Wernicke's: Functional Mapping of Ancillary Language Centers Prior to Brain Tumor Surgery. *Tomography* 2023;9:1254-1275
11. Fisicaro RA, Jost E, Shaw K, et al. Cortical Plasticity in the Setting of Brain Tumors. *Top Magn Reson Imaging* 2016;25:25-30
12. Lee MH, Smyser CD, Shimony JS. Resting-state fMRI: a review of methods and clinical applications. *AJNR Am J Neuroradiol* 2013;34:1866-1872
13. Matthews PM, Honey GD, Bullmore ET. Applications of fMRI in translational medicine and clinical practice. *Nat Rev Neurosci* 2006;7:732-744
14. Nichols TE, Das S, Eickhoff SB, et al. Best practices in data analysis and sharing in neuroimaging using MRI. *Nat Neurosci* 2017;20:299-303
15. Black DF, Vachha B, Mian A, et al. American Society of Functional Neuroradiology-Recommended fMRI Paradigm Algorithms for Presurgical Language Assessment. *AJNR Am J Neuroradiol* 2017;38:E65-E73
16. Diaz MT, Hernandez A. The multifaceted nature of language across adulthood. *Brain Lang* 2022;230:105125
17. Binder JR, Frost JA, Hammeke TA, et al. Human brain language areas identified by functional magnetic resonance imaging. *J Neurosci* 1997;17:353-362
18. Benjamin CF, Walshaw PD, Hale K, et al. Presurgical language fMRI: Mapping of six critical regions. *Hum Brain Mapp* 2017;38:4239-4255
19. Petrella JR, Shah LM, Harris KM, et al. Preoperative functional MR imaging localization of language and motor areas: effect on therapeutic decision making in patients with potentially resectable brain tumors. *Radiology* 2006;240:793-802
20. Yarkoni T, Poldrack RA, Nichols TE, et al. Large-scale automated synthesis of human functional neuroimaging data. *Nat Methods* 2011;8:665-670
21. Lee J, Kumar VA, Teo JM, et al. Comparative analysis of brain language templates with primary language areas detected from presurgical fMRI of brain tumor patients. *Brain Behav* 2024; Accepted March 2024
22. Cox RW. AFNI: software for analysis and visualization of functional magnetic resonance neuroimages. *Comput Biomed Res* 1996;29:162-173
23. Gorgolewski K, Burns CD, Madison C, et al. Nipype: a flexible, lightweight and extensible neuroimaging data processing framework in python. *Front Neuroinform* 2011;5:13
24. Rolls ET, Huang CC, Lin CP, et al. Automated anatomical labelling atlas 3. *Neuroimage* 2020;206:116189
25. Fonov V, Evans AC, Botteron K, et al. Unbiased average age-appropriate atlases for pediatric studies. *Neuroimage* 2011;54:313-327
26. Avants BB, Tustison NJ, Song G, et al. A reproducible evaluation of ANTs similarity metric performance in brain image registration. *Neuroimage* 2011;54:2033-2044
27. Price CJ. A review and synthesis of the first 20 years of PET and fMRI studies of heard speech, spoken language and reading. *Neuroimage*

2012;62:816-847

28. Chang EF, Raygor KP, Berger MS. Contemporary model of language organization: an overview for neurosurgeons. *J Neurosurg* 2015;122:250-261
29. Barnett A, Marty-Dugas J, McAndrews MP. Advantages of sentence-level fMRI language tasks in presurgical language mapping for temporal lobe epilepsy. *Epilepsy Behav* 2014;32:114-120
30. Labache L, Joliot M, Saracco J, et al. A SENtence Supramodal Areas AtlaS (SENSAAS) based on multiple task-induced activation mapping and graph analysis of intrinsic connectivity in 144 healthy right-handers. *Brain Struct Funct* 2019;224:859-882
31. Li Y, Li P, Yang QX, et al. Lexical-Semantic Search Under Different Covert Verbal Fluency Tasks: An fMRI Study. *Front Behav Neurosci* 2017;11:131
32. Hayama HR, Rugg MD. Right dorsolateral prefrontal cortex is engaged during post-retrieval processing of both episodic and semantic information. *Neuropsychologia* 2009;47:2409-2416
33. Unadkat P, Fumagalli L, Rigolo L, et al. Functional MRI Task Comparison for Language Mapping in Neurosurgical Patients. *J Neuroimaging* 2019;29:348-356
34. Botha H, Mantyh WG, Murray ME, et al. FDG-PET in tau-negative amnestic dementia resembles that of autopsy-proven hippocampal sclerosis. *Brain* 2018;141:1201-1217
35. Pieperhoff P, Sudmeyer M, Dinkelbach L, et al. Regional changes of brain structure during progression of idiopathic Parkinson's disease - A longitudinal study using deformation based morphometry. *Cortex* 2022;151:188-210
36. Branco P, Seixas D, Castro SL. Mapping language with resting-state functional magnetic resonance imaging: A study on the functional profile of the language network. *Hum Brain Mapp* 2020;41:545-560
37. Gil N, Lipton ML, Fleysher R. Registration quality filtering improves robustness of voxel-wise analyses to the choice of brain template. *Neuroimage* 2021;227:117657
38. Chen HS, Kumar VA, Johnson JM, et al. Effect of brain normalization methods on the construction of functional connectomes from resting-state functional MRI in patients with gliomas. *Magn Reson Med* 2021;86:487-498
39. Friedman L, Glover GH, Krenz D, et al. Reducing inter-scanner variability of activation in a multicenter fMRI study: role of smoothness equalization. *Neuroimage* 2006;32:1656-1668
40. Karambelkar A, Gandhi A, Trunz L, et al. National medicare trends in the utilization of fMRI. *Neuroscience Informatics* 2022;2

Supplementary Table 1: Patient demographic and clinical characteristics

Characteristic	No. of patients
Age (mean) (range) (yr)	51 ± 16 (18-87)
Sex	
Male	184
Female	133
Hand dominance	
Right	253
Mixed	25
Left	30
N.A.	9
Tumor location	
Medial frontal	2
Left frontal	108
Left parietal	25
Left temporal	91
Left occipital	1
Left insula	21
Left frontal-parietal	6
Left frontal-temporal	7
Left parietal-temporal	8
Left parietal-occipital	2
Left temporal-occipital	3
Left frontal-parietal-temporal	1
Left parietal-temporal-occipital	1
Left intraventricular	1
Right frontal	15
Right parietal	5
Right temporal	7
Right occipital	1
Right insula	8
Right frontal-temporal	2
Right frontal-parietal-temporal	1
N.A.	1
Pathology	
Glioblastoma	139
Astrocytoma	
Grade III	33
Grade II	47
Grade I	1
Grade Unassigned	2
Oligodendroglioma	
Grade III	19
Grade II	25
Grade Unassigned	1
Meningioma	

Grade II	1
Grade I	2
Glioma	
Grade III	2
Grade II	3
Grade Unassigned	1
Brain metastases	32
Choroid plexus carcinoma	
Grade III	1
Dysembryoplastic neuroepithelial tumor	
Grade I	1
CNS lymphoma	1
Mesenchymal tumor	1
Others	2
N.A.	3

Supplementary Table 2. Language-related ROIs and their Automated Anatomical Labelling Atlas 3 Counterparts

Respective left and right hemisphere counterparts from Automated Anatomical Labelling Atlas 3 were applied for analyses in left and right language-related regions-of-interest (ROIs) in this study.

Language-related ROI	**Automated Anatomical Labelling Atlas 3 Regions (labels)**
Anterior Primary Language Area (aPLA)	Inferior frontal gyrus, opercular part (L:7, R:8) Inferior frontal gyrus, triangular part (L:9, R:10)
Temporal Posterior Primary Language Area ($pPLA_T$)	Superior temporal gyrus (L:85, R:86) Middle temporal gyrus (L:89, R:90)
Parietal Posterior Primary Language Area ($pPLA_P$)	Supramarginal gyrus (L:67, R:68) Angular gyrus (L:69, R:70)
Supplementary Motor Area (SMA)	Supplementary motor area (L:15, R:16)
Dorsolateral Prefrontal Cortex (DLPFC)	Middle frontal gyrus (L:5, R:6)
Basal Temporal Language Area (BTLA)	Parahippocampal gyrus (L:43, R:44) Fusiform gyrus (L:59, R:60) Inferior temporal gyrus (L:93, R:94)
Insula	Insula (L:33, R:34)